FISEVIER

Contents lists available at ScienceDirect

Chemical Engineering Journal

journal homepage: www.elsevier.com/locate/cej



Multi-porous quaternized chitosan/polystyrene microbeads for scalable, efficient heparin recovery



Hamed Eskandarloo, Mary Godec, Mohammad Arshadi, Olga I. Padilla-Zakour, Alireza Abbaspourrad*

Department of Food Science, College of Agriculture & Life Sciences, Cornell University, 243 Stocking Hall, Ithaca, NY 14853, USA

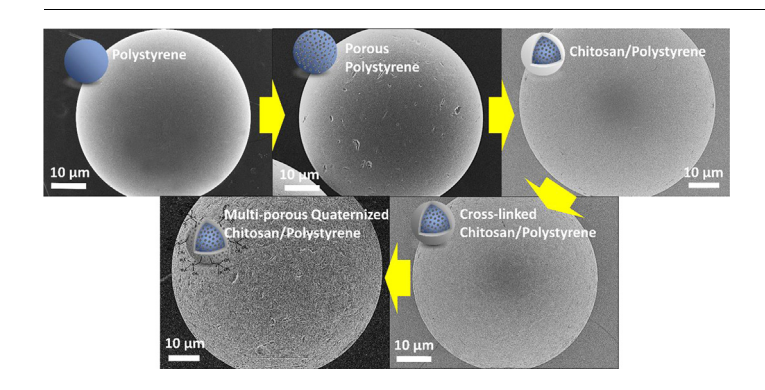
HIGHLIGHTS

- Novel porous polystyrene supported chitosan-coated microbeads were fabricated.
- Quaternary ammonium groups were grafted on the functional groups of chitosan
- The microbeads were then made multi-porous using a solvent/non-solvent treatment.
- Microbeads were used for the efficient and selective recovery of heparin.
- The adsorption efficiency of microbeads was significantly higher than Amberlite.

ARTICLE INFO

Keywords: Heparin Scale-up purification Chitosan Polystyrene beads Quaternary ammonium Selective capture

GRAPHICAL ABSTRACT



ABSTRACT

Heparin is a commercially valuable polysaccharide used as an anticoagulant for surgical procedures. However, it is difficult to isolate at high concentrations from the complex tissues from which it is derived. To address this problem, we fabricated novel porous polystyrene (PS) supported chitosan (CS)-coated microbeads by electrostatic assembly for the efficient, scalable, and selective recovery of heparin. These CS/PS microbeads were further reacted and quaternized using glycidyltrimethylammonium chloride to improve their heparin adsorption efficiency at high pH values. Additionally, a tetrahydrofuran/n-heptane treatment was used to introduce multiporosity throughout the quaternized-CS/PS microbead structure, increasing the functional surface area. Scanning electron microscopy was used to evaluate the effects of pre- and post-treatments on the bead surface morphology. The adsorption efficiency of the CS/PS microbeads vs. Amberlite FPA98 Cl resin, a commercially available adsorbent, was evaluated as a function of pH (4.1-9.2). Heparin adsorption was demonstrated to improve with both the introduction of a multi-porous bead structure and the quaternization of the CS/PS microbeads to provide a pH-independent cationic polyelectrolyte character. We also demonstrated that the CS/PS microbeads could be effectively regenerated using a saturated NaCl solution and used for repeated heparin recovery without significant adsorption capacity loss. Moreover, multi-porous quaternized-CS/PS microbeads selectively adsorbed heparin in the presence of bovine serum albumin at pH 9 by adding 0.5 M NaCl to screen electrostatics between the CS and proteins. In addition, microbeads selectively adsorbed heparin in a real sample, composed of a mixture of biological solution containing heparin isolated from porcine intestinal mucosa.

E-mail address: alireza@cornell.edu (A. Abbaspourrad).

^{*} Corresponding author.

1. Introduction

Heparin is a linear, unbranched, and highly sulfated polysaccharide, which is composed of alternating units of sulfated uronic acid and D-glucosamine. It has a high density of negative charge due to the presence of sulfonate and carboxylic groups in its polysaccharide structure [1,2]. Heparin performs a range of important biological functions and is widely used for its anticoagulant properties in applications such as the treatment of deep vein thrombosis and systemic embolism syndrome, as well as the pre-operative prevention of blood clotting [3,4]. Additionally, it exhibits anti-inflammatory and anti-viral properties, and can also inhibit cancer cell growth and delay the onset of Alzheimer's disease symptoms [5,6].

Although heparin can be extracted from a variety of tissues, including intestine, lung, and liver, commercial production typically uses porcine intestinal mucosa [7]. The initial extraction results in crude, partially-purified heparin [8]. Through autolysis or chemical digestion, the heparin is then released from mast cells and proteoglycans [9]. However, the concentration in the autolyzed starting material is very low ($\sim 0.01\%$ w/w). Hence, a recovery step must be used to selectively capture and isolate the heparin from complex tissue to enable further purification. To do so, early protocols applied a high concentration of ammonium sulfate at a low pH (2-2.5) to capture heparin in this autolyzed material [10,11]. However, this method most likely precipitates primarily protein-bound heparins rather than free molecules, as proteolytic (trypsin) digestion is conducted after the acid precipitation step in established commercial protocols. This is supported by the observation that unrefined heparin obtained after acidic precipitation still features high amounts of protein [12]. These proteins in the crude product may give rise to serious losses of heparin in purification methods. Moreover, it was also reported that acid precipitation does not recover all heparin in the sample. This is most likely because nonprotein-bound heparin does not precipitate under these conditions [13].

Other capture methods utilize hydrophobic primary amines whose positive charges allow the formation of insoluble complexes with heparin under slightly acidic conditions [9]. Ammonium cation capture is currently the most broadly utilized technique for recovery of this compound from digestion mixtures. However, more recent methods employ quaternized ammonium cations, generally either immobilized on a resin [14,15] or designed in such a way that they selectively form insoluble complexes with heparin (i.e., quaternary ammonium salts) [16,17]. Both strategies exploit the polymeric nature and unique high charge density of heparin (~3.7 negative charges/disaccharide), distinguishing it from other biopolymers present in the digestion mixture [18], which permits strong charge-based cooperative binding.

Polycation polymers are good candidates for the adsorption of negatively charged sulfated polysaccharides. The polycation chitosan (CS) is one such potential adsorbent, due to its high amino content. CS, the second most abundant biopolymer in nature, is a biodegradable and biocompatible polysaccharide produced from the deacetylation of chitin [18]. CS has been successfully used in the past for selective capture of sulfated polysaccharides through electrostatic interactions between its own protonated –NH₂ groups and the negatively charged –SO₄ $^-$ groups of the polysaccharides [19–22]. In some studies, quaternary ammonium groups have been grafted on the functional groups of CS to improve the adsorption capability at high pH values [23–25].

However, the true challenge for traditional CS-based adsorbents is the difficulty in recycling them for reuse in industrial applications. The fabrication of micro-sized CS-based adsorbents is a possible alternative to traditional CS, nanoparticle or solution form, because micro-sized adsorbents are easier to collect and reuse. However, such adsorbents also have a low adsorption capacity and rate due to their relatively large size and low specific surface area, which limits their applicability for large industrial systems [26].

To address these issues, we propose a new strategy for the fabrication of quaternized chitosan/polystyrene (CS/PS) microbeads with a

multi-porous structure for selective adsorption of heparin. In this strategy, the sulfonated porous-structure of the PS beads was used as the support for a CS thin-film, deposited on the surface by the electrostatic force between the $-\mathrm{NH}_2$ groups of CS and the $-\mathrm{SO}_3\mathrm{H}$ groups of PS. The CS coating was then cross-linked by glutaraldehyde to improve its chemical stability. Next, the CS–NH $_2$ groups were quaternized to produce permanent positive charges along the polymer chains, resulting in a pH-independent cationic polyelectrolyte character. The resulting quaternized-CS/PS microbeads were then made multi-porous using a solvent/non-solvent treatment, in which porosity is featured throughout the interior and exterior of the bead structure [27], maximizing the functionally-coated specific surface area and resulting in increased adsorption ability.

We evaluated the heparin adsorption efficiency of these multiporous quaternized-CS/PS microbeads and compared their adsorption efficiency to the commercially available adsorbent Amberlite FPA98 Cl resin. A model heparin-bovine serum albumin (BSA) mixture was used to evaluate the selectivity of heparin capture with the proposed system. The multi-porous quaternized-CS/PS microbeads demonstrate higher adsorption efficiency than the current commercial method and can be used as an efficient adsorbent for the selective capture of heparin.

2. Materials and methods

2.1. Materials

Analytical-reagent grade chitosan (> 75% deacetylation, high molecular weight, 310,000-375,000 Da), glutaraldehyde (aqueous solution, 25 wt%), glycidyltrimethylammonium chloride (GTMAC) $(\ge 90\%)$, acetic acid $(0.5 \,\mathrm{M})$, tetrahydrofuran (THF, $0.2 \,\mathrm{M})$, *n*-heptane (0.5 M), concentrated sulfuric acid (98%), methylene blue, hydrochloric acid (0.1 M), sodium hydroxide (0.1 M), sulfuric acid (0.1 M), butanol, and ethanol were purchased from Sigma Aldrich. The anion exchange resin, Amberlite FPA98 Cl, comprising a cross-linked PS matrix with quaternary ammonium groups, was provided by Dow Chemical, U.S. Heparin sodium salt, from porcine intestinal mucosa, was obtained from Celsus Laboratories (Cincinnati, USA). Polystyrene beads (PS beads) were supplied by iFilters Co. (Ontario, USA). A mixture of biological solution containing heparin isolated from porcine intestinal mucosa (500 mg L⁻¹) was provided by Shineway Co. (WH Group, China). Physical and chemical characteristics of the PS beads are given in Table 1. Fig. S1 of the Supporting Information displays a scanning electron microscopy (SEM) image of the PS microbeads (diameter distribution shown in the inset). Observations revealed that the microbeads were spherical in shape, with an average size of $\sim 500 \, \mu m$.

Table 1
Physical and chemical characteristics of the PS beads.

8% Cross-linked poly(styrene-co-Polymer matrix structure: divinylbenzene) Physical form and appearance: Brownish yellow - brown, amber Functional Groups: R-SO₃ Ionic form: Na ⁺ 0.3-1.2 mm Particle size range Moisture retention: 46-50% 8-10% Swelling (Na⁺ \rightarrow H⁺) Specific gravity (moist form): 1.27 120 °C* Operating temperature: pH range stability: 0 - 14

^{*} Insoluble in dilute or moderately concentrated acids, alkalis, and in all common solvents.

^{**} Thermally stable to higher than 120 $^{\circ}\text{C}$ in alkali's such as, sodium or alkaline earth like calcium and magnesium salt forms.

2.2. Fabrication of multi-porous quaternized-CS/PS beads

2.2.1. Pre-treatment of PS beads

Sulfonated porous PS beads were fabricated using a solvent/non-solvent treatment [27], followed by sulfonation with concentrated sulfuric acid [28]. Briefly, for the preparation of the porous bead structure, 500 mg of PS microbeads were transferred into a 20 mL DI-water/butanol solution (1:1 v/v). Then, a 6 mL THF/n-heptane mixture at a volumetric ratio of 5:1 was added to this solution, which was heated at 60 °C for 6 h. Next, the beads were separated by decanting and repeatedly washed with ethanol. The porous PS beads were then sulfonated using 10 mL concentrated sulfuric acid heated to 40 °C under magnetic stirring for 24 h. After dilution with DI-water, the PS microbeads were repeatedly washed with ethanol and then dried at 35 °C for 24 h. Previous work has shown that the PS surface after sulfonation remains negatively charged in a wide pH range (2–12) [29].

2.2.2. CS coating onto the surface of the PS beads

First, the CS solution was prepared by dissolving CS powder into $100\,\text{mL}$ of 1% (v/v) acetic acid aqueous solution (pH \sim 3). Next, the sulfonated porous PS microbeads were added to this CS solution under magnetic stirring and maintained at 30 °C for 24 h. The weight ratio of CS to PS was in the range of 0.6 to 1. The microbeads were then collected and thoroughly washed with DI water. Glutaraldehyde was added into a 50 mL CS/PS suspension in DI-water to improve the chemical stability of the CS film on the PS surface. This cross-linking reaction occurred under magnetic stirring at 50 °C for 24 h. The range of weight ratios of glutaraldehyde to CS/PS microbeads tested was 0.1 to 1. The obtained cross-linked CS/PS beads were collected and repeatedly washed with DI water to remove water-soluble impurities.

2.2.3. Quaternization of CS/PS beads

At high pH values (pH > 7), characteristic of heparin extraction from tissue, the selectivity of heparin adsorption was found to be low. To address this issue and improve the adsorption efficiency, we functionalized the CS coating with GTMAC by adding the CS/PS microbeads to a 50 mL aqueous acetic acid solution at a pH of $\sim\!6$, followed by dropwise addition of GTMAC. The weight ratio of GTMAC to CS/PS was 30 to 1. The solution was mixed by a magnetic stirrer for 5 h at 55 °C. Finally, the beads were collected and repeatedly washed with ethanol, then dried at 25 °C for 24 h.

2.2.4. Formation of the porous surface structure

The porous surface structure of the quaternized-CS/PS microbeads was formed by the same procedure as in Section 2.2.1 for the formation of the porous bead structure. A schematic diagram of these series of steps for the fabrication of multi-porous quaternized-CS/PS microbeads is shown in Scheme 1.

A set of preliminary experiments was carried out to evaluate and optimize the effect of these fabrication parameters in terms of the heparin adsorption efficiency of the resulting multi-porous quaternized-CS/PS microbeads, including different weight ratios of CS to PS, coating time of CS onto PS, reaction temperature of CS coating onto PS, pH of CS coating onto PS, glutaraldehyde to CS/PS, and GTMAC to CS/PS, the volume ratio of THF/n-heptane, and the THF/n-heptane treatment time (Table 2). The results are shown in Fig. S2 of the Supporting Information. These preliminary results allowed us to identify the most appropriate conditions for the fabrication of multi-porous quaternized-CS/PS microbeads with high adsorption efficiency, utilizing the following conditions: 0.6:1 as the weight ratio of CS to PS, 24h for the coating time of CS onto PS, 30 °C for the reaction temperature of CS coating onto PS, 3 for the pH of CS coating onto PS, 0.1:1 as the weight ratio of glutaraldehyde to CS/PS, 30:1 as the weight ratio of GTMAC to CS/PS, 5 mL as the volume of THF, and 6 h for the THF/n-heptane treatment time of the microbeads.

2.3. Characterization

The surface morphology and size distribution of the microbeads were observed using a field-emission SEM (LEO FESEM, LEO 1550). Fourier-transform infrared (FT-IR) spectra were recorded from 4000 to $400~{\rm cm}^{-1}$ on a Shimadzu FTIR Model-IRAffinity-1S (MIRacle 10). 128 scans were taken at a resolution of $2~{\rm cm}^{-1}$. The zeta potential was measured at 25 °C using a Zeta Sizer Nano-ZS system, Nano Series (Malvern, United Kingdom). Each zeta potential value was averaged from three consecutive measurement series of 20 runs each.

2.4. Adsorption experiments

We added 250 mg of the CS/PS microbeads to a 50 mL aqueous solution of heparin (20 mg L⁻¹) to study the material's absorption capabilities. The mixed solution was then shaken at 25 °C. At selected times (10, 20, 30, 40, and 50 min), we removed a 5 mL sample from the aqueous solution using a syringe filter and measured the heparin concentration in the supernatant using the methylene-blue-assisted spectrophotometric method [30,31]. Methylene blue is a cationic metachromatic dye with an affinity for polyanions, such as heparin. In brief, 1 mL of the heparin solution was added to 1 mL of methylene blue (10 mg L⁻¹). Then the solution was mixed using a vortex mixer for five minutes, and the absorbance was measured by UV-vis spectrophotometer (Shimadzu, UV-2600) on the basis of the intensity of the 663 nm band, which corresponds to free methylene blue molecules. In the presence of heparin, methylene blue molecules form dimers absorbing at 567 nm, and λ_{max} at 663 nm decreases due to the decreasing concentration of free methylene blue, as shown in Fig. S3 of the Supporting Information. A standard curve plotting absorbance vs. concentration of methylene blue was made. The concentration of free methylene blue in solution was estimated from the standard curve and subtracted from the total amount of methylene blue added to determine the heparin concentration in solution. The equilibrium heparin adsorption capacity of the adsorbents (mg/g) was calculated from the following equation:

$$q_e = \frac{(C_0 - C_e) \times V}{m} \tag{1}$$

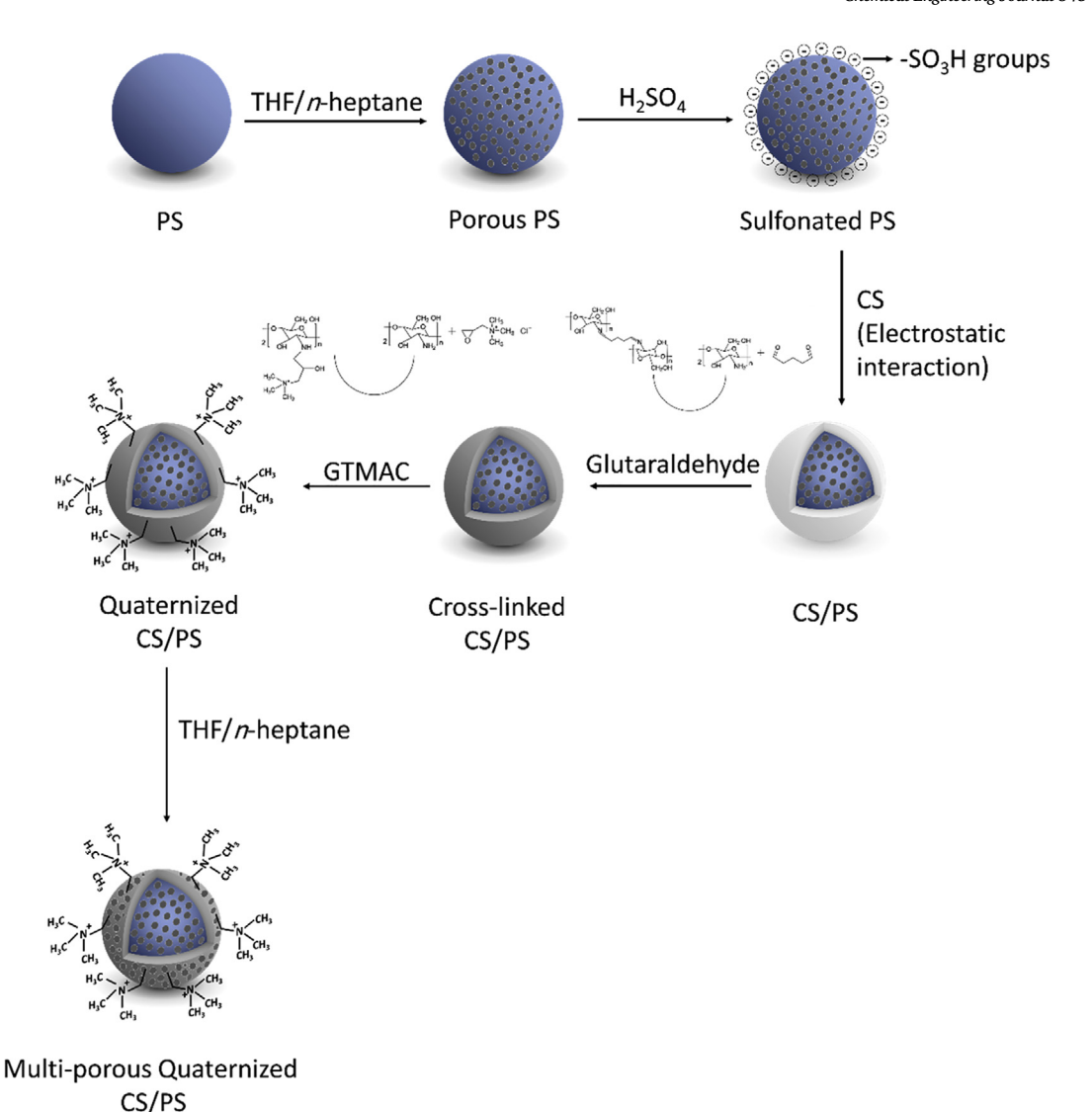
in which $q_{\rm e}$ is the amount of heparin adsorbed per unit weight of the microbeads (mg/g), $C_{\rm 0}$ and $C_{\rm e}$ are the initial and equilibrium concentration of heparin, respectively, V is the volume of the heparin aqueous solution (L), and m is the weight of the adsorbent microbeads (g).

A model heparin-BSA mixture containing $20\,\mathrm{mg\,L^{-1}}$ of each component was used to evaluate the selectivity of heparin capture with the proposed system. The BSA concentration in the mixture supernatant was measured using the acid oxidation spectrophotometric method [21]. In brief, a 0.3 mL sample of the mixture supernatant was removed and transferred into 3 mL of a 90% (v/v) sulfuric acid solution, which was then shaken fully using a vortex mixer, then placed into a water bath of 90 °C for 10 min under stirring. The solution was cooled to room temperature and kept for an additional 30 min, then BSA concentrations were determined with UV–vis spectrophotometer (Shimadzu, UV-2600) at 280 nm.

The concentration of heparin in real sample tests was quantified using a heparin ELISA kit (MyBiosource, San Diego, CA, USA) by measuring absorbance changes at 450 nm on a SpectraMax iD3 Multi-Mode Microplate Reader (Molecular Devices; Sunnyvale, CA). The real sample was a mixture of biological solution containing heparin isolated from the porcine intestinal mucosa. Initial heparin concentration in the digestion mixture was 500 mg $\rm L^{-1}$.

2.5. Regeneration of CS/PS microbeads

In regeneration studies, the heparin-loaded CS/PS microbeads were



Scheme 1. Schematic diagram of the fabrication of multi-porous quaternized-CS/PS microbeads.

Table 2The reaction variables for the fabrication of multi-porous quaternized-CS/PS microbeads with optimal values.

Reaction variable	Variation range	Optimal value
CS:PS (w/w)	0.1:1-0.9:1	0.6:1
CS coating time (h)	2-48	24
CS coating temperature (°C)	30-60	30
CS coating pH	3–6	3
Glutaraldehyde:CS/PS (w/w)	0.05:1-0.4:1	0.1:1
GTMAC:CS/PS (w/w)	15:1-35:1	30:1
Volume of THF (mL)	1-5	5
THF/n-heptane treatment time (h)	1–6	6

treated with 5% NaCl at 40 °C for 30 min. Then, the microbeads were additionally shaken with saturated NaCl at 50 °C for 3 h, causing heparin to desorb from the microbeads' surfaces. Afterwards, the microbeads were separated from the mixture and rinsed with DI-water. Five consecutive adsorption-desorption cycles were performed to study the stability and reusability of the CS/PS microbeads.

All the experiments were carried out three times in order to determine the variability of the results and to assess the experimental errors. Results shown in the Figs. 4 and 6 are the averages of normalized data from three experiments, and error bars indicate standard deviation

of the measurements.

3. Results and discussion

3.1. Characterization

We studied the influences of pre- and post-treatments on the surface morphology of the PS microbeads using SEM (Fig. 1). When the PS microbeads (Fig. 1a) were initially treated with a mixture of THF/nheptane, dissolution and migration of the copolymer chains occurred [27], resulting in a porous surface structure as shown in Fig. 1b. When the PS microbeads were added into the solution of CS, a thin-film of CS gradually adsorbed onto the surface due to electrostatic interactions between the $-NH_2$ groups of CS and the $-SO_3H$ groups of PS. Fig. 1c shows that this procedure resulted in the deposition of a non-uniform film of CS onto the surface of the porous PS microbeads. Increasing the concentration of CS relative to the PS microbeads resulted in increased coating thickness (Fig. S4 of the Supporting Information). After crosslinking CS on the PS microbeads by glutaraldehyde, the surface of the peripheral CS shell became smoother (Fig. 1d). SEM imaging showed that the reaction of CS/PS microbeads with GTMAC resulted in no discernable effect on the surface structure. Finally, the multi-porous surface structure of the CS/PS microbeads was achieved by a secondary THF/n-heptane treatment (Fig. 1e).

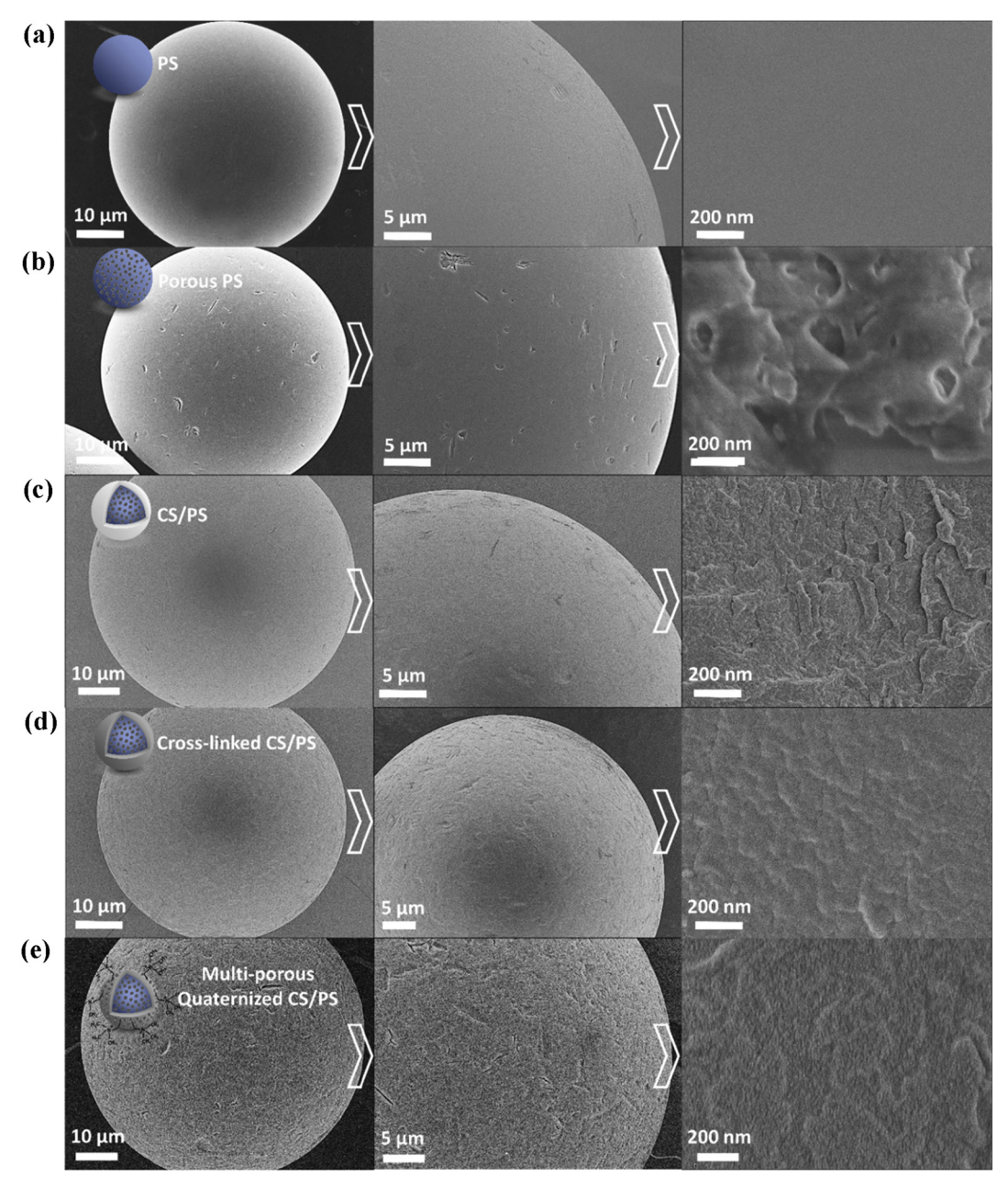


Fig. 1. SEM micrographs of (a) PS, (b) porous PS, (c) CS/PS, (d) cross-linked CS/PS, and (e) multi-porous quaternized-CS/PS microbeads. To the right are magnified views, showing the surface morphology of the microbeads.

The sulfonated PS microbeads were studied using FT-IR. Fig. 2a shows the FT-IR spectra of the PS microbeads before and after sulfonation. The appearance of characteristic peaks at 100-1200 cm⁻¹ indicates that the microbeads were significantly sulfonated. Additionally, the –OH stretching derivatives band at $\sim 3400 \, \mathrm{cm}^{-1}$ for the sulfonated microbeads was broadened. Cross-linking of bulk CS through the formation of imine bonds between CS and glutaraldehyde was also confirmed by FT-IR (Fig. 2b). In the FT-IR spectrum of the cross-linked-CS, the band at 1633 cm $^{-1}$ representing a C = N bond, which appears due to the formation of the imine group by the Schiff-base reaction of the amine group of CS and the aldehydic group of glutaraldehyde. The reaction of the primary amino group of bulk CS with the glycidyl group of GTMAC was also confirmed by FT-IR analysis (Fig. 2b). In the FT-IR spectrum of quaternized-CS, the band at $1483\,\mathrm{cm}^{-1}$ can be attributed to an asymmetric angular bending of the -CH3 groups on the quaternary group. This band is absent in the FT-IR spectrum of CS. In addition, the band at 1560 cm⁻¹, attributed to the -NH₂ groups that are present in the FT-IR spectrum of CS, is much weaker in the quaternized-CS spectrum due to the substitution of the $-\mathrm{NH}_2$ groups. These imaging and spectroscopic results verify that the synthetic strategy used was able to successfully fabricate PS microbeads with a quaternized-CS thin-film and porous structure.

3.2. Heparin adsorption

We added the CS/PS microbeads to aqueous solutions of heparin to study the material's adsorption capability by following the changes in heparin concentration using a colorimetric method with methylene blue as the titrant. Fig. 3 shows the dependence of the heparin concentration relative to its initial value ($C_{\rm t}/C_0$) as a function of time and at different pH (4.9–9.2) in the presence of different adsorbents, including CS/PS, quaternized-CS/PS, and multi-porous quaternized-CS/PS, in comparison with a commercially available adsorbent, Amberlite FPA98 Cl resin. The insets of Fig. 3 show the equilibrium adsorption capacity

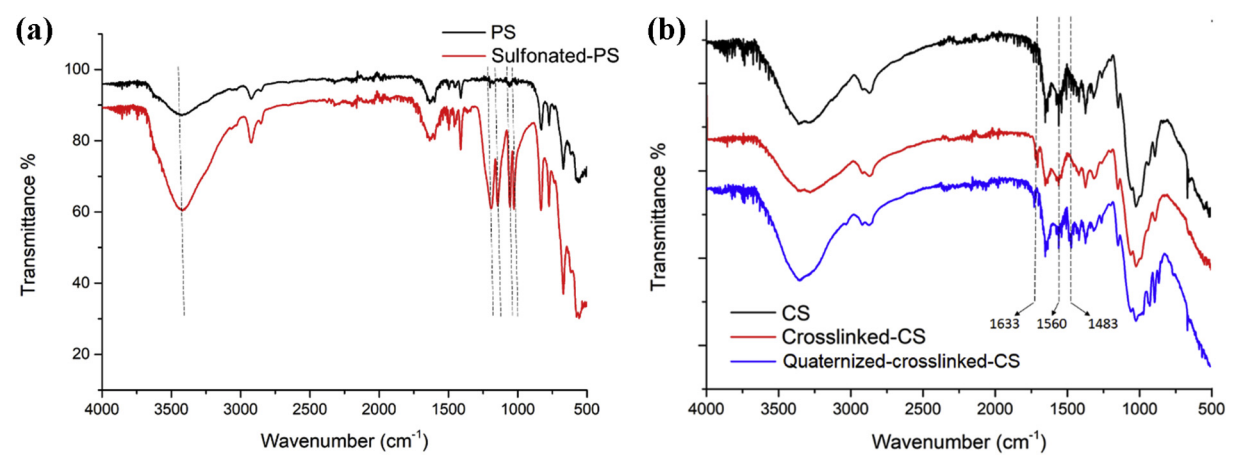


Fig. 2. FT-IR spectra of (a) PS and sulfonated-PS microbeads and (b) bulk CS, cross-linked-CS, and quaternized-CS.

(qe, mg/g) of heparin for the different adsorbents. The adsorption efficiency of the CS/PS microbeads toward heparin, both in terms of the adsorption rate and the amount of heparin adsorbed per unit weight of microbeads (*i.e.*, the adsorption capacity), was drastically decreased by increasing the pH value. At pH 4.9, 61% of heparin was adsorbed after 30 min by the CS/PS microbeads, while at pH 7.6 and 9.2, only 43% and 7% of heparin, respectively, was adsorbed by that same time. Similar results were also found by others [19], in that the heparin adsorption efficiency of bulk CS decreased with increasing pH value. This

decreasing adsorption efficiency of CS/PS microbeads at increasing pH could be due to the deprotonation of the $\mathrm{NH_3}^+$ (or $\mathrm{NH_2}^+$) groups on the surface of the CS/PS microbeads, decreasing the active sites available for binding negatively charged heparin molecules.

In contrast, quaternized-CS/PS microbeads showed better adsorption performance as compared to CS/PS microbeads throughout the whole pH range studied (Fig. 3). The improved adsorption efficiency for quaternized-CS/PS microbeads, especially at high pH values, could be due to the functionalization of CS with N-quaternized [-+N(CH₃)₃]

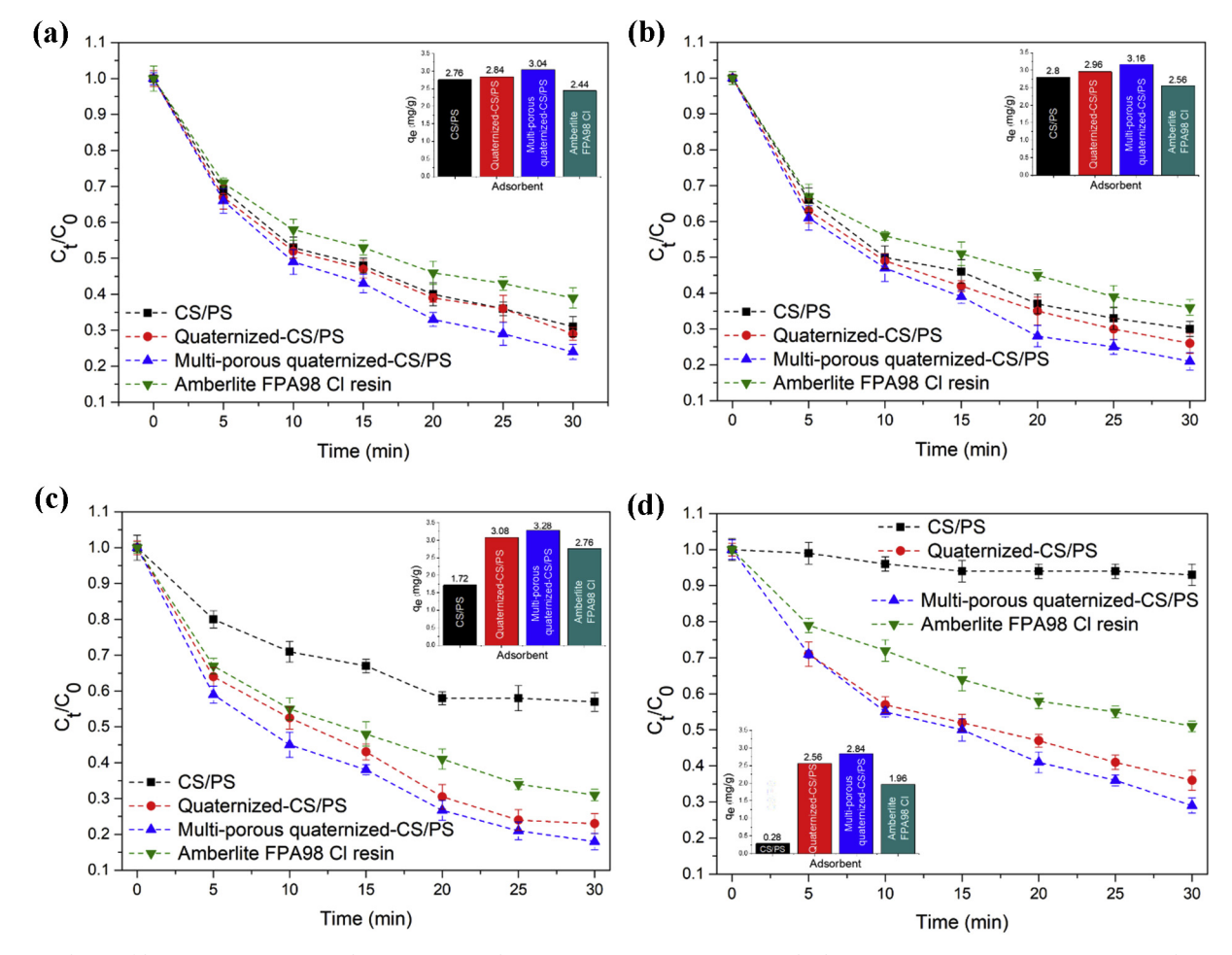


Fig. 3. Dependence of heparin concentration relative to its initial concentration (C_t/C_0) on time and adsorption capacity $(q_e, mg/g)$ (insets) in the presence of different adsorbents as a function of pH: (a) 4.9; (b) 6.1; (c) 7.6; and (d) 9.2. Initial heparin concentration was 20 mg L⁻¹.

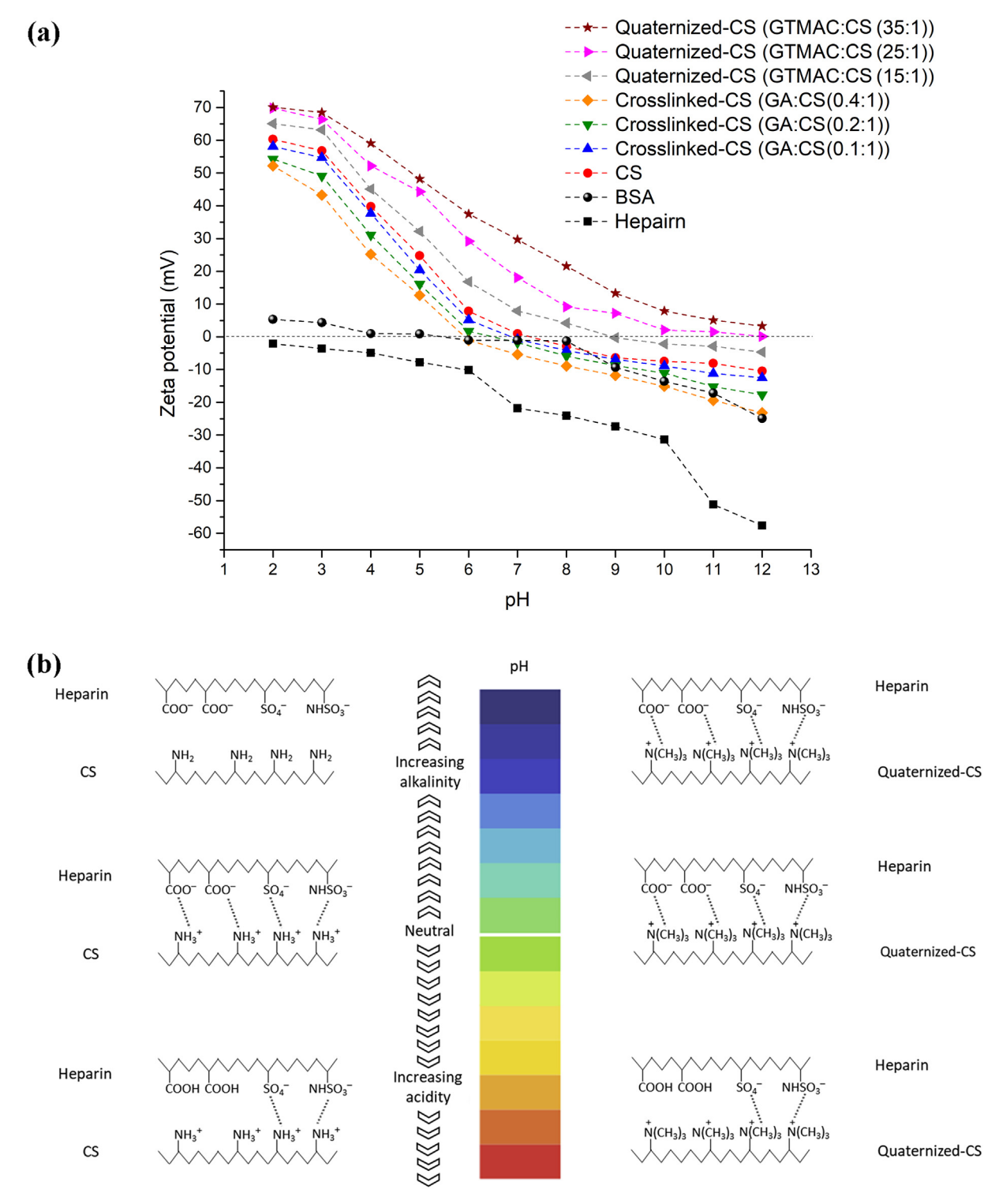


Fig. 4. (a) Zeta potential of bulk CS, CS-derivatives, heparin, and BSA as a function of pH. (b) Schematic illustration of possible interactions between CS and quaternized-CS with heparin as a function of pH.

groups, which do not undergo pH-dependent de-protonation. Therefore, a positive charge is maintained on the surface of the quaternized-CS/PS microbeads, even at higher pH values.

The results also demonstrated the advantage of a multi-porous bead structure, which can improve adsorption efficiency because of the higher surface-to-volume ratio that provides more available reactive sites (Fig. 3). At pH 9.2, 64% and 51% of heparin was adsorbed after 30 min with the quaternized-CS/PS and Amberlite FPA98 Cl resin, respectively. The heparin adsorption increased to nearly 71% at pH 9.2

with the use of multi-porous quaternized-CS/PS microbeads. The adsorption capacity for CS/PS, quaternized-CS/PS, multi-porous quaternized-CS/PS, and Amberlite FPA98 Cl resin, after 30 min at pH 9.2 was 0.28, 2.56, 2.84, and 1.96 mg/g, respectively. These results strongly indicate that the multi-porous quaternized-CS/PS microbeads possess an excellent adsorption capacity, which can be applied to industrial scale capture of heparin.

To study the electrostatic interactions between bulk CS and heparin, we measured their surface charges at a wide pH range (2-12) in terms

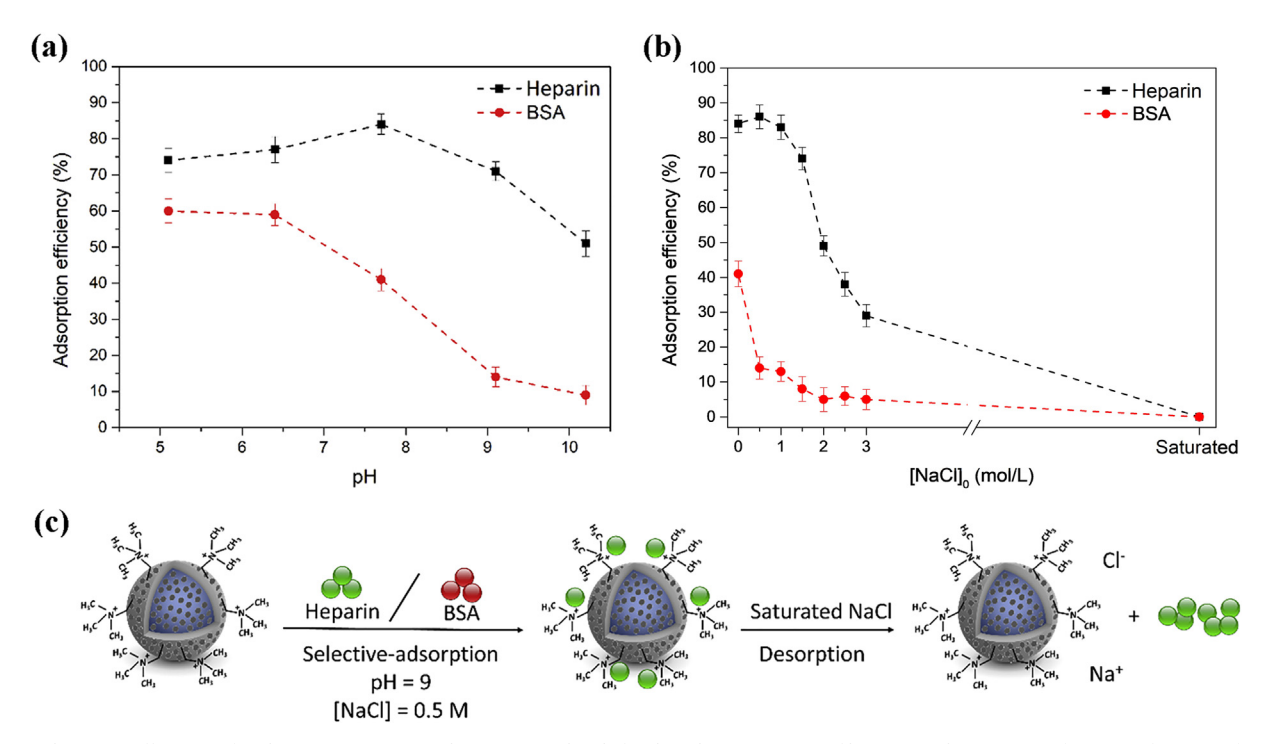


Fig. 5. (a) Adsorption efficiency of multi-porous quaternized-CS/PS microbeads for the selective capture of heparin in the presence of BSA as a function of pH. Initial heparin and BSA concentrations were 20 mg L^{-1} . (b) The effect of NaCl on the selective capture of heparin in the presence of BSA as a function of NaCl concentration. Initial heparin and BSA concentrations were 20 mg L^{-1} , pH = 7.7. (c) Schematic illustration of the selective adsorption-desorption of heparin by multi-porous quaternized-CS/PS microbeads.

of zeta potentials (Fig. 4a). Heparin had a negative zeta potential for all pH investigated. Although it is a multifunctional polyanion, which also bears carboxyl groups, its numerous sulfate groups are permanently ionized throughout the whole pH range [32]. Thus, heparin behaves essentially as a strong polyanion. However, the zeta potential of bulk CS was positive at low pH values (< 7.1) due to the protonation of $-NH_2$ groups but became negative at higher pH values (> 7.1), showing an isoelectric point at pH 7.1. The zeta potential values decreased when the CS was cross-linked with glutaraldehyde. For CS cross-linked with 0.4:1 (w/w) of glutaraldehyde to CS, the zeta potential became negative for pH > 5.9, showing about -6.4 mV of zeta potential at pH 7.1. The positive zeta potential of CS decreased by cross-linking, which may be due to the reduced number of free amino groups. As expected, the zeta potential of quaternized-CS was significantly higher than that for CS, resulting from the presence of positively charged N-quaternized [-*N (CH₃)₃] groups along the polymer chain. At pH 7.1 the quaternary amino groups in quaternized-CS were protonated, while the deprotonated -NH2 groups in CS were in equilibrium with the protonated groups. The zeta potential of quaternized-CS increased with increasing quaternization rate (increasing the weight ratio of GTMAC to CS), due to the higher degree of substitution, consistent with prior studies [20,33]. As can be seen in Fig. 4a, the zeta potential of the quaternized-CS (GTMAC to CS (w/w) of 25:1 and 35:1) remained positive throughout the whole pH range investigated. Therefore, negatively charged heparin can be adsorbed easily onto the quaternized-CS surface via electrostatic interactions at high pH values. A schematic illustration of the possible interactions between CS and quaternized-CS with heparin as a function of pH is shown in Fig. 4b.

The presence of proteins in solution can decrease the efficiency of heparin capture due to the competition of protein and heparin molecules for the same sites on the adsorbent surface, or because of complexation of protein and heparin molecules in solution, which may adsorb less onto the adsorbent surface due to steric effects [34]. As shown in Fig. 4a, the BSA showed an isoelectric point at pH 5.3, while heparin remained negatively charged in all pH values investigated.

Heparin behaves as a strong polyanion with a high charge density. It can complex with BSA at lower pH, and especially below the BSA isoelectric point [32]. Therefore, selective adsorption of heparin in the presence of BSA can only occur at pH higher than 5.

Fig. 5a shows the competitive adsorption of heparin and BSA onto the surface of multi-porous quaternized-CS/PS microbeads as a function of pH. When the pH exceeded 6.4, the adsorption of BSA began to decrease. We noted that the adsorption efficiency of BSA suddenly decreased when the pH value was higher than 6.4 and decreased to only 14% for pH 9.1, at which point the strong adsorption of heparin by the microbeads was still retained at 71%. It has been reported that at pH 6.5-7.0 the intrinsic binding constants of BSA to heparin markedly decrease with an increase in pH, due to the increasing negative charge of BSA and the resultant increasing repulsion between the molecules [21]. As can be seen at pH 6.4-7.7 the adsorption of BSA onto the microbeads sharply decreased but without a change in heparin adsorption, indicating the increasing electrostatic repulsion between heparin and BSA, along with a strong electrostatic interaction between heparin and the multi-porous quaternized-CS/PS material. Thus, the selective capture of heparin in the presence of BSA could be readily achieved by controlling the pH of the solution.

In principle, salt concentration can strongly influence the interactions of polyanion-polycation pairs [35]. We evaluated the effect of ionic strength on the adsorption of heparin and BSA onto multi-porous quaternized-CS/PS microbeads with the addition of NaCl (0.5–3 M) at pH 9 (Fig. 5b). With an increase in the concentration of NaCl within this range, the adsorption of BSA was significantly decreased. However, the heparin adsorption did not change until the NaCl concentration exceeded 1.5 M, demonstrating the good selectivity of the microbeads for heparin adsorption against BSA in the range of 0.5–1.5 M NaCl. Accordingly, based on the strong electrostatic interaction between the highly negatively charged heparin and the positively charged multiporous quaternized-CS/PS microbeads, we were able to control the solution pH containing NaCl to achieve selective capture for heparin in the presence of proteins. A schematic illustration of the selective

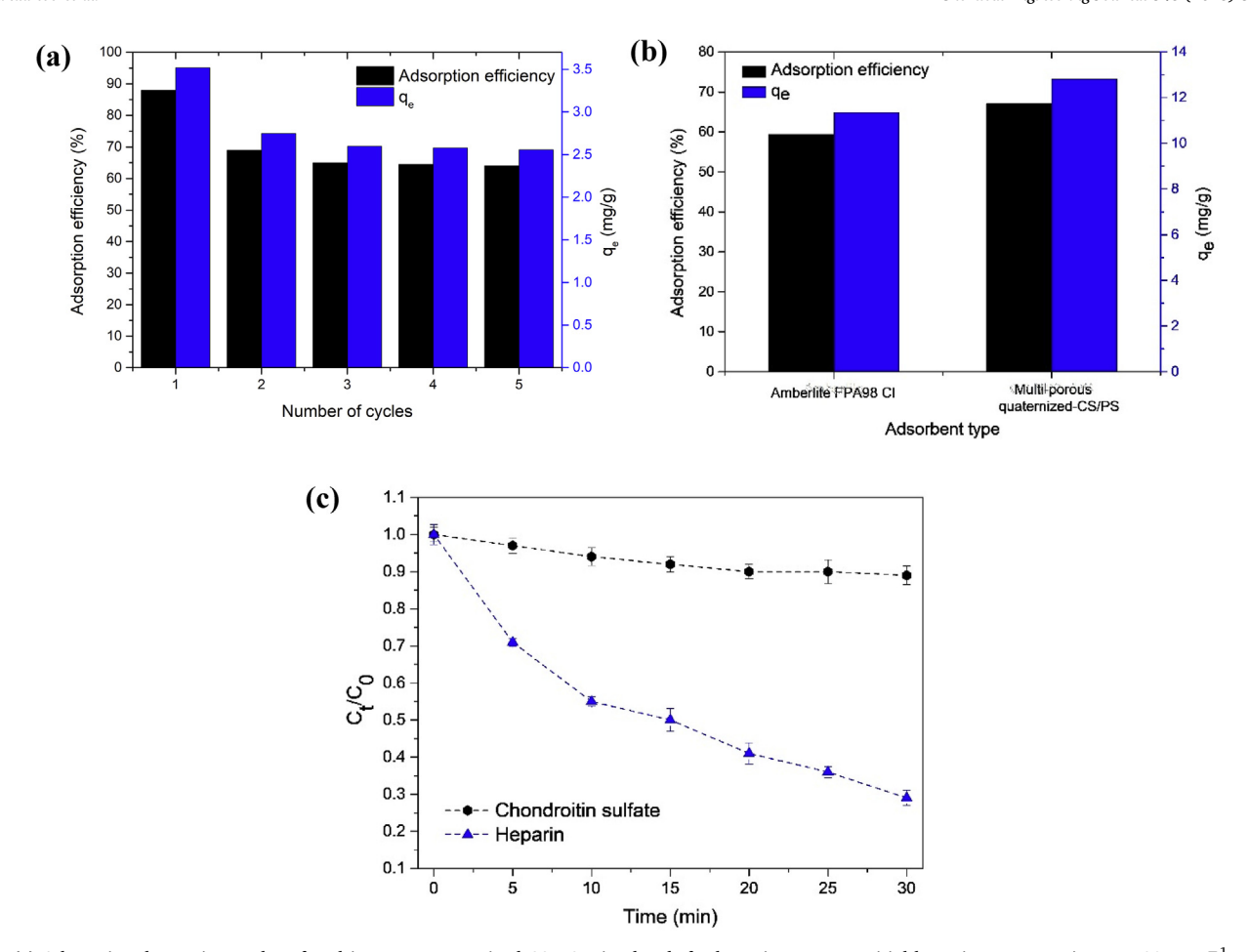


Fig. 6. (a) Adsorption-desorption cycles of multi-porous quaternized-CS/PS microbeads for heparin capture. Initial heparin concentration was 20 mg L^{-1} , pH = 9. (b) Adsorption capacity (q_e , mg/g) and adsorption efficiency (%) of heparin in the real sample onto the multi-porous quaternized-CS/PS microbeads vs. Amberlite FPA98 Cl resin. Initial heparin concentration in the digestion mixture was 500 mg L^{-1} , the adsorbent dosage was 320 mg, and the pH = 9. (c) Dependence of chondroitin sulfate and heparin concentrations relative to their initial concentration (C_t/C_0) on time in the presence of the multi-porous quaternized-CS/PS microbeads. Initial chondroitin sulfate and heparin concentrations were 20 mg L^{-1} (pH = 9.2).

adsorption and desorption of heparin by the multi-porous quaternized-CS/PS microbeads is shown in Fig. 5c.

We also studied the stability and reusability of the multi-porous quaternized-CS/PS microbeads, as it is an important factor for practical applications (Fig. 6a). Our results showed that the adsorption capacity of heparin on the microbeads decreased slowly after several cycles of adsorption and desorption. Between each cycle, the microbeads were treated with saturated NaCl by the procedure given in Section 2.5. After regeneration, the microbeads were reused in the adsorption of fresh heparin solution. The adsorption capacity of fresh microbeads was 3.52 mg/g. Under the same conditions, the adsorption capacity of microbeads in the 2nd and 5th adsorption runs was 2.75 and 2.56 mg/g, respectively. At the end of five regeneration cycles, the adsorption capacity remained at 72.8% of the initial value. These results indicated that the multi-porous quaternized PS-supported CS microbeads can be recycled for heparin adsorption using saturated NaCl. This confirms the reusability and stability of the adsorbent produced in the study. In addition, the size of the microbeads enables easier collection for reuse compared to nano-sized particles typically used in industrial adsorption

Fig. 6b shows the equilibrium adsorption capacity (q_e , mg/g) and adsorption rate (%) of heparin onto the multi-porous quaternized-CS/PS microbeads ν s. Amberlite FPA98 Cl resin in the real sample. The real sample was a mixture of biological solution containing heparin isolated from porcine intestinal mucosa. The results clearly confirm that in the real sample the adsorption efficiency of heparin onto CS/PS

microbeads, both in terms of the adsorption rate and the adsorption capacity, was higher than the Amberlite FPA98 Cl resin. In addition, the specificity of the multi-porous quaternized-CS/PS microbeads toward other types of potential interfering agents (e.g., chondroitin sulfate, as a sulfated glycosaminoglycan, which can also be present in practical feedstocks) was studied (Fig. 6c). We found that the CS/PS microbeads have a very low adsorption capacity (0.44 mg/g) and rate (11%) toward chondroitin sulfate (30 min exposure time at pH 9.2). However, under the same conditions, the adsorption capacity and rate of the microbeads for heparin were 2.84 mg/g and 71%, respectively. The results reveal the high adsorption specificity of the fabricated microbeads toward heparin.

Besides efficient activity and environmental friendliness, economic cost can also determine whether a new system can be used practically. Therefore, we estimated the cost of the CS/PS microbeads and compared it with that of Amberlite FPA98 Cl resin. The PS microbeads are based on a low-cost resin with a commercial price of \$5/kg. The preliminary calculations showed that the cost of the post-modifications, using CS and GTMAC, was approximately \$12–20/kg. In total, this price is significantly lower than the Amberlite FPA98 Cl resin (\$135/kg), which is a commercially available adsorbent for heparin from Dow Chemical. Therefore, CS/PS microbeads are inexpensive and easy to prepare in large quantities, providing the opportunity to use this adsorbent in selective, scalable recovery of heparin from mixtures of biological solutions.

4. Conclusion

In this study, we describe a new strategy for the fabrication of a CS/ PS micro-sized adsorbent with a multi-porous structure and quaternized-CS thin-film for the selective capture of heparin. Sulfonated porous-structured PS microbeads (mean particle size 500 µm) were used as the support and a CS thin-film was successfully formed (CS:PS, 0.6:1 (w/w)) by the electrostatic interaction between the CS-NH $_2$ and PS-SO₃H groups. Glutaraldehyde (GA:CS/PS, 0.1:1 (w/w)) crosslinking was employed to improve the chemical stability of the CS coating. The amino groups were subsequently quaternized to provide permanent positive charges along the polymer chains, resulting in a pHindependent cationic polyelectrolyte character. The desired final multiporous structure was achieved using a 6 h THF/n-heptane (5:1 (v/v)) treatment. For each step in this fabrication process, we evaluated the comparative heparin adsorption efficiency of the materials in comparison with a commercially available adsorbent (Amberlite FPA98 Cl resin). The quaternized-CS/PS microbeads with multi-porous structure showed the highest heparin adsorption efficiency, both in terms of the rate of adsorption (71%) and adsorption capacity (2.84 mg/g), during 30 min time at pH 9.2. Due to the unique advantages afforded by the surface structure and the useful properties of the quaternary ammonium groups, the adsorption rate for multi-porous quaternized-CS/PS microbeads was significantly higher compared to that of the nonmodified CS/PS microbeads, non-porous quaternized-CS/PS microbeads, and Amberlite. The selectivity of the modified microbeads was assayed with the separation of heparin from a model heparin-BSA mixture at a range of pH and NaCl concentrations. Moreover, CS/PS microbeads selectively adsorbed heparin in a real sample, containing a mixture of biological solution with heparin isolated from porcine intestinal mucosa. The results showed that the multi-porous quaternized-CS/PS microbeads can be used as an efficient adsorbent for the pHindependent recovery of heparin at large scale.

Acknowledgments

This work made use of the Cornell Center for Materials Research's Shared Facilities, which are supported through the NSF MRSEC program (DMR-1719875). This publication was made possible by research funding provided by Shineway company (WH Group).

Appendix A. Supplementary data

Supplementary data associated with this article can be found, in the online version, at http://dx.doi.org/10.1016/j.cej.2018.04.099.

References

- S. Boddohi, C.E. Killingsworth, M.J. Kipper, Polyelectrolyte multilayer assembly as a function of pH and ionic strength using the polysaccharides chitosan and heparin, Biomacromolecules 9 (2008) 2021–2028.
- [2] J.C. Lee, X.A. Lu, S.S. Kulkarni, Y.S. Wen, S.C. Hung, Synthesis of heparin oligosaccharides, J. Am. Chem. Soc. 126 (2004) 476–477.
- [3] Z. Xiao, B.R. Tappen, M. Ly, W. Zhao, L.P. Canova, H. Guan, R.J. Linhardt, Heparin mapping using heparin lyases and the generation of a novel low molecular weight heparin, J. Med. Chem. 54 (2010) 603–610.
- [4] I. Wijesekara, R. Pangestuti, S.K. Kim, Biological activities and potential health benefits of sulfated polysaccharides derived from marine algae, Carbohydr. Polym. 84 (2011) 14–21.
- [5] M. Lima, T. Rudd, E. Yates, New applications of heparin and other glycosaminoglycans, Molecules 22 (2017) 749–759.
- [6] J. Men, J. Guo, W. Zhou, N. Dong, X. Pang, B. Gao, Preparation of cationic functional polymer poly (Acryloxyethyltrimethyl ammonium chloride)/SiO₂ and its adsorption characteristics for heparin, Korean J. Chem. Eng. 34 (2017) 1889–1895.
- [7] T.W. Barrowcliffe, History of heparin, in: R. Lever, B. Mulloy, C.P. Page (Eds.),

- Heparin-A Century of Progress, Springer Berlin/Heidelberg, Germany, 2012.
- [8] R. Sasisekharan, Z. Shriver, From crisis to opportunity: a perspective on the heparin crisis, Thromb Haemost 102 (2009) 854–858.
- [9] J.Y. van der Meer, E. Kellenbach, L.J. van den Bos, From farm to pharma: an overview of industrial heparin manufacturing methods, Molecules 22 (2017) 1025–1037.
- [10] A.F. Charles, D.A. Scott, Studies on heparin: observations on the chemistry of heparin, Biochem. J. 30 (1936) 1927–1933.
- [11] M.H. Kruizenga, L.B. Spaulding, The preparation of highly active barium salt of heparin and its fractionation into two chemically and biologically different constituents, J. Biol. Chem. 148 (1943) 641–647.
- [12] J.D.H. Homan, J. Lens, A simple method for the purification of heparin, Biochim. Acta 2 (1948) 333–337.
- [13] J.A. Bush, S. Freeman, E.B. Hagerty, Process for preparing heparin, U.S. Patent 2, 884, 358, 22 April 1957.
- [14] C.C. Griffin, R.J. Linhardt, C.L. van Gorp, T. Toida, R.E. Hileman, R.L. Schubert, S.E. Brown, Isolation and characterization of heparan sulfate from crude porcine intestinal mucosal peptidoglycan heparin, Carbohydr. Res. 276 (1995) 183–197.
- [15] F.A.E. Van Houdenhoven, A.L.M. Sanders, P.J.J. van zuthpen, Process for the purification of heparin, U.S. Patent 6, 232, 093, 3 January 2000.
- [16] G. Nomine, B. Pierre, Process of purifying heparin, and product produced therefrom, U.S. Patent 2, 989, 438, 20 June 1961.
- [17] M.M. Mozen, T.D. Evans, Process for purifying heparin. U.S. Patent 3, 058, 884, 14 September 1959.
- [18] M. Bodnar, J.F. Hartmann, J. Borbely, Preparation and characterization of chitosanbased nanoparticles, Biomacromolecules 6 (2005) 2521–2527.
- [19] K. Kaminski, K. Zazakowny, K. Szczubiałka, M. Nowakowska, pH-sensitive genipincross-linked chitosan microspheres for heparin removal, Biomacromolecules 9 (2008) 3127–3132.
- [20] K. Kamiński, K. Szczubiałka, K. Zazakowny, R. Lach, M. Nowakowska, Chitosan derivatives as novel potential heparin reversal agents, J. Med. Chem. 53 (2010) 4141–4147.
- [21] X. Wei, J. Duan, X. Xu, L. Zhang, Highly efficient one-Step purification of sulfated polysaccharides via chitosan microspheres adsorbents, ACS Sustainable Chem. Eng. 5 (2017) 3195–3203.
- [22] U. Bhaskar, A.M. Hickey, G. Li, R.V. Mundra, F. Zhang, L. Fu, C. Cai, Z. Ou, J.S. Dordick, R.J. Linhardt, A purification process for heparin and precursor polysaccharides using the pH responsive behavior of chitosan, Biotechnol. Progr. 31 (2015) 1348–1359.
- [23] S. Rosa, M.C. Laranjeira, H.G. Riela, V.T. Fávere, Cross-linked quaternary chitosan as an adsorbent for the removal of the reactive dye from aqueous solutions, J. Hazard. Mater. 155 (2008) 253–260.
- [24] C. Yu, J. Geng, Y. Zhuang, J. Zhao, L. Chu, X. Luo, Y. Zhao, Y. Guo, Preparation of the chitosan grafted poly (quaternary ammonium)/Fe₃O₄ nanoparticles and its adsorption performance for food yellow 3, Carbohydr. Polym. 152 (2016) 327–336.
- [25] Y. Xie, S. Li, G. Liu, J. Wang, K. Wu, Equilibrium, kinetic and thermodynamic studies on perchlorate adsorption by cross-linked quaternary chitosan, Chem. Eng. J. 192 (2012) 269–275
- [26] C. Chen, J. Hu, D. Xu, X. Tan, Y. Meng, X. Wang, Surface complexation modeling of Sr (II) and Eu (III) adsorption onto oxidized multiwall carbon nanotubes, J. Colloid Interface Sci. 323 (2008) 33–41.
- [27] T. Zha, L. Song, P. Chen, W. Nie, Y. Zhou, Nonsolvent/solvent-induced phase separation to multi-porous sulfonated polystyrene/chitosan/silver particles and their application in adsorbing chromium ion (III) and reduction of methylene blue, Colloids Surf., A 481 (2015) 423–430.
- [28] W. Jiang, X. Chen, B. Pan, Q. Zhang, L. Teng, Y. Chen, L. Liu, Spherical polystyrenesupported chitosan thin film of fast kinetics and high capacity for copper removal, J. Hazard. Mater. 276 (2014) 295–301.
- [29] W. Jiang, X. Chen, Y. Niu, B. Pan, Spherical polystyrene-supported nano-Fe₃O₄ of high capacity and low-field separation for arsenate removal from water, J. Hazard. Mater. 243 (2012) 319–325.
- [30] K.T. Al-Jamal, W.T. Al-Jamal, K. Kostarelos, J.A. Turton, A.T. Florence, Anti-angiogenic poly-L-lysine dendrimer binds heparin and neutralizes its activity, Results Pharma Sci. 2 (2012) 9–15.
- [31] M. Jakubowska, J. Adamus, J. Gębicki, A. Marcinek, A. Sikora, Pulse radiolysis and spectrophotometric studies on the binding of organic cations with heparin, Radiat. Phys. Chem. 99 (2014) 6–11.
- [32] M. Houska, E. Brynda, Interactions of proteins with polyelectrolytes at solid/liquid interfaces: sequential adsorption of albumin and heparin, J. Colloid Interface Sci. 188 (1997) 243–250.
- [33] Y. Gao, Z. Zhang, L. Chen, W. Gu, Y. Li, Synthesis of 6-N, N, N-trimethyltriazole chitosan via "click chemistry" and evaluation for gene delivery, Biomacromolecules 10 (2009) 2175–2182.
- [34] D.T.H. Wassell, G. Embery, Adsorption of chondroitin-4-sulphate and heparin onto titanium: effect of bovine serum albumin, Biomaterials 18 (1997) 1121–1126.
- [35] T.T. Ho, K.E. Bremmell, M. Krasowska, D.N. Stringer, B. Thierry, D.A. Beattie, Tuning polyelectrolyte multilayer structure by exploiting natural variation in fucoidan chemistry, Soft Matter. 11 (2015) 2110–2124.